Flexural strengthening of RC T-beams using varied NSM-CFRP configurations

Y. Haryanto
Department of Civil Engineering, Universitas Jenderal Soedirman, Purwokerto, Indonesia.
National Center for Research on Earthquake Engineering, Taipei, Taiwan.
Department of Civil Engineering, National Cheng Kung University, Tainan, Taiwan.

L. Nugroho & H.-T. Hu
Department of Civil Engineering, National Cheng Kung University, Tainan, Taiwan.

F.-P. Hsiao, P.-W. Weng & C.-C. Lin
National Center for Research on Earthquake Engineering, Taipei, Taiwan.

B.A. Hidayat
Department of Civil Engineering, National Cheng Kung University, Tainan, Taiwan.
Department of Civil Engineering, Universitas Diponegoro, Semarang, Indonesia.

ABSTRACT

This study investigated the flexural strengthening of reinforced concrete (RC) T-beams using the near-surface mounted (NSM) method, with carbon fiber-reinforced polymer (CFRP) rods embedded at varying depths. Experimental tests were conducted to evaluate the flexural performance of the strengthened beams in the negative moment region. When comparing fully-embedded (BF-D) and half-embedded (BH-D) CFRP rods with a control beam (BN-D) under high-rate cyclic loading, significant increases in ultimate load capacity were observed—21.23% for BH-D and 30.86% for BF-D—despite instances of debonding. However, this approach resulted in reduced ductility and an increased tendency toward brittle failure. Additionally, a rate-dependent material formula was developed and validated, which accurately predicted the flexural strength of the negative moment region, with results in good agreement with the experimental findings.

1 INTRODUCTION

Reinforced concrete (RC) members often require strengthening, and carbon fiber-reinforced polymer (CFRP) materials are preferred due to their lightweight nature, corrosion resistance, and high tensile strength. CFRP's superior tensile strength makes it particularly effective in the tensile zone, which is why it is commonly used for the flexural strengthening of RC beams to accommodate additional flexural and tensile forces. The near-surface mounted (NSM) method is frequently employed for CFRP strengthening in RC structures. This method involves embedding CFRP rods or plates into grooves within the concrete cover, offering protection for the CFRP against potential damage while preserving the structure's appearance.

Tests on beam specimens have shown that the application of NSM-CFRP strips or rods significantly enhances the load-bearing capacity and stiffness of the beams (Hassan and Rizkalla, 2002; Zhang et al., 2022; Shakary et al., 2012). According to ACI 440.2R standards (ACI Committee 440, 2017), a groove depth of at least 1.5 times the rod diameter is required for the full embedding of CFRP rods and effective stress transfer. However, older buildings often have insufficient concrete cover thickness, which may limit the ability to achieve the minimum groove depth. Haryanto et al. (2022) demonstrated that partially embedded CFRP rods can still significantly improve beam capacity. The successful implementation of this technique in structures depends on appropriate installation methods, groove preparation, and the proper compaction of the epoxy bonding agent.

Cyclic load testing reveals structural performance in terms of tensile cracking, compressive failure, fatigue resistance, energy dissipation, stiffness degradation, and recovery. Under non-reversed cyclic loading, Han et al. (2022) observed that the ultimate load increased for beams strengthened in the negative moment region with half-embedded and fully-embedded NSM-CFRP rods. Additionally, these beams demonstrated improved energy dissipation capabilities (Haryanto et al., 2023). Building on this work, Haryanto et al. (2022) investigated strengthened RC T-beams under reversed cyclic loading. Their findings showed that the strengthened beams exhibited enhanced load-carrying capacity and reduced stiffness degradation, along with improved energy absorption. However, an increased tension reinforcement ratio resulted in a decrease in ductility.

Most studies on CFRP-strengthened RC beams have focused on their static behavior under slow or static loading rates. However, RC structures are typically subjected to various dynamic stresses, including seismic activity. The response of RC elements to loading rates depends on the mechanical properties of the materials used. This research involved an experimental investigation of RC T-beams strengthened with NSM-CFRP rods in the negative moment region. The study examined the behavior of NSM-CFRP strengthened specimens with varying embedment depths of CFRP rods under reversed cyclic loads at high loading rates, simulating dynamic loading conditions.

2 EXPERIMENTAL CAMPAIGN

2.1 Design of specimens

The three RC T-beam specimens had the following dimensions: a length of 2600 mm, an overall depth of 300 mm, and a flange width of 600 mm. The web measured 150 mm in width and 180 mm in depth, with a flange depth of 120 mm. The reinforcement included two steel rebars, each with a diameter of 16 mm, placed in both the tension and compression zones. Additionally, 10 mm diameter steel stirrups were installed at 175mm spacing to provide shear reinforcement. The detailed strengthening configurations are shown in Figure 1.

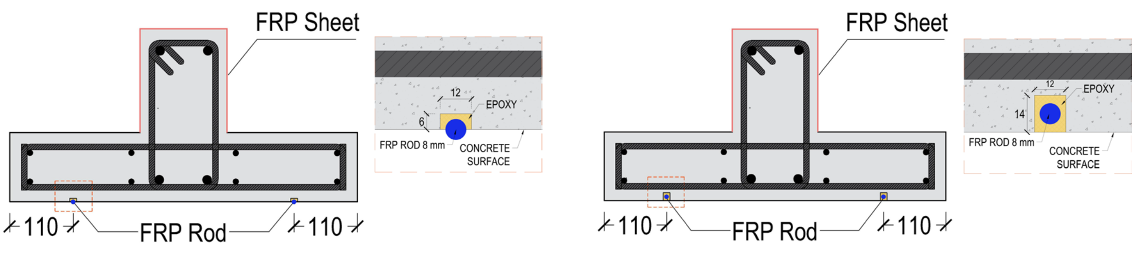

(a) (b)

Figure 1: Strengthening configurations (unit: mm): (a) SB-H specimen, (b) SB-F specimen

At 28 days, two beams were strengthened with 100 mm wide CFRP sheets installed at 130 mm intervals and two 8-mm-diameter CFRP rods. The main difference between the strengthened beams was the embedment depth of the rods: one beam featured fully embedded rods (SB-F), while the other had rods embedded to the midpoint (SB-H). For comparison, a reference beam (RB) without CFRP sheets or rods was included in the tests. For the strengthened specimens, grooves were cut into the concrete cover of the flange to house the rods, which were secured with epoxy. The CFRP sheets were precisely cut and bonded to the webs of the beams using epoxy in accordance with design specifications.

2.2 Characteristics of materials

Uniaxial testing revealed that the D10 reinforcement bars had a yield stress (f_y) of 350.67 MPa and an ultimate stress (f_u) of 500.85 MPa. The D16 bars demonstrated a yield stress (f_y) of 492.25 MPa and an ultimate stress (f_u) of 727.51 MPa. Concrete cylinders with a diameter of 150 mm and a height of 300 mm were cast during the fabrication process. Structural testing indicated a compressive strength of 27.46 MPa for the concrete.

2.3 Loading protocol

A three-point bending test was performed on the beams using a reverse cyclic loading protocol at a high loading rate of 0.5 m/s (Adhikary, 2012), with a clear span of 2300 mm. Each displacement stage included two loading cycles, and the displacement amplitude was incrementally increased by 10% of the control beam's maximum displacement, as determined from monotonic testing and based on a prior study (Haryanto et al., 2022). The loading protocol employed is shown in Figure 2.

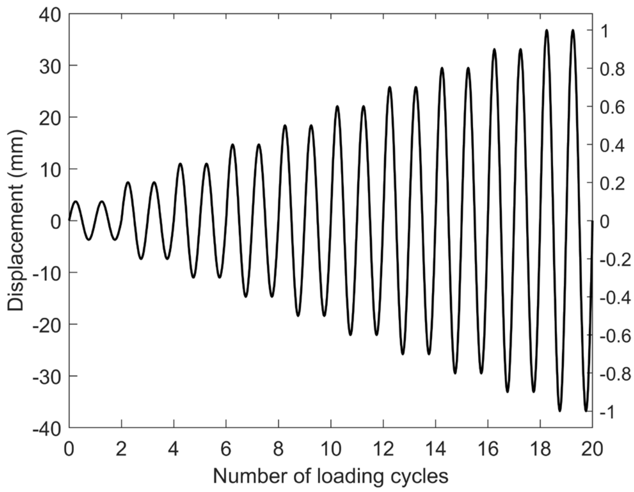

Figure 2. High-rate cyclic loading applied at the middle span of the specimen

3 RESULTS AND DISCUSSION

3.1 Hysteresis responses and failure modes

Figure 3 illustrates the hysteresis responses of the RB, SB-H, and SB-F specimens. The skeleton curve derived from the hysteresis loops was generated to analyse the performance of the beams. The ultimate load values obtained from the curves for RB, SB-H, and SB-F are 176.63 kN, 214.13 kN, and 231.14 kN, respectively. These results indicate an improvement of 21.23% for SB-H and 30.86% for SB-F relative to RB. During the descending phase following the peak load, the SB-H beam was unable to sustain or delay the reduction in load due to early slip and partial debonding, which occurred at a displacement of 29.50 mm.

Figure 4 displays the failure modes associated with each specimen. Cracks initially developed near the midspan and propagated through the entire section, leading to the yielding of the reinforcement. In the SB-H specimen, debonding of CFRP rods occurred while the SB-F specimen displayed only cracks in the bottom of the beam, which inhibited the visual identification of debonding. The RB beam exhibited considerable spalling and crushing of the concrete, whereas the strengthened beams demonstrated minimal spalling of the concrete cover in the midspan region, which might be attributed to the increased shear capacity and confinement provided by the CFRP sheets.

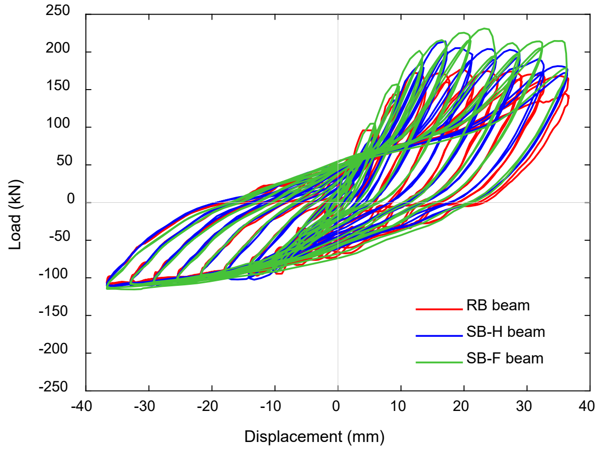

(a)

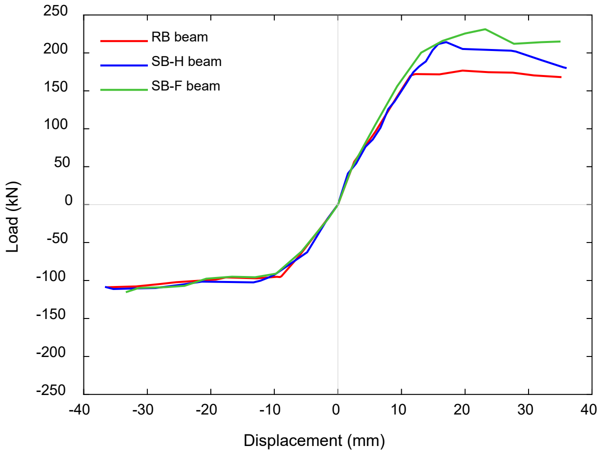

(b)

Figure 3: Response of all beams under high-rate cyclic loading: (a) hysteresis curves, (b) skeleton curves

(a)

(b)

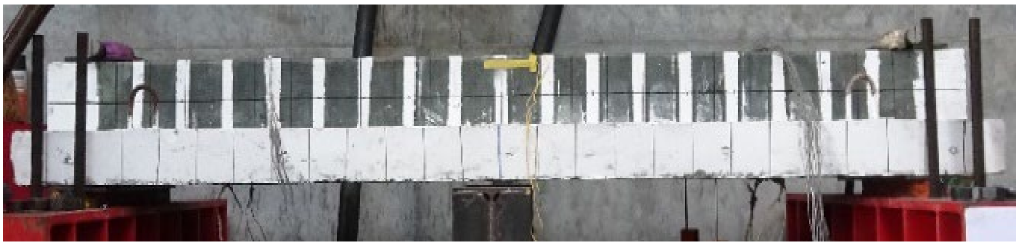

(c)

Figure 4: Failure modes: (a) RB specimen, (b) SB-H specimen, (c) SB-F specimen

3.2 Stiffness degradation and energy dissipation

Figure 5(a) presents a comparison of stiffness degradation relative to displacement. In the negative moment region, all beams showed a significant decrease in stiffness at 7.40 mm, followed by a consistent degradation rate up to 14.70 mm. Beyond 14.70 mm, continued crack propagation and concrete crushing in the RB specimen led to greater stiffness degradation in the SB-H and SB-F specimens compared to RB. Despite this, the stiffness of the strengthened beams remained higher than that of the control beam throughout all displacement stages. At 18.50 mm, the SB-H and SB-F beams exhibited similar stiffness; however, the SH beam experienced a gradual reduction in stiffness due to early slip and debonding.

Figure 5(b) illustrates that the cumulative energy dissipation at each displacement stage during cyclic loading was highly similar among all specimens up to the 18.40 mm stage. However, the reference beam (RB) demonstrated a lower energy absorption capacity compared to the strengthened beams. Specifically, the SB-F and SB-H beams achieved energy dissipation rates that were 15.08% and 10.57% higher than that of the RB beam, respectively.

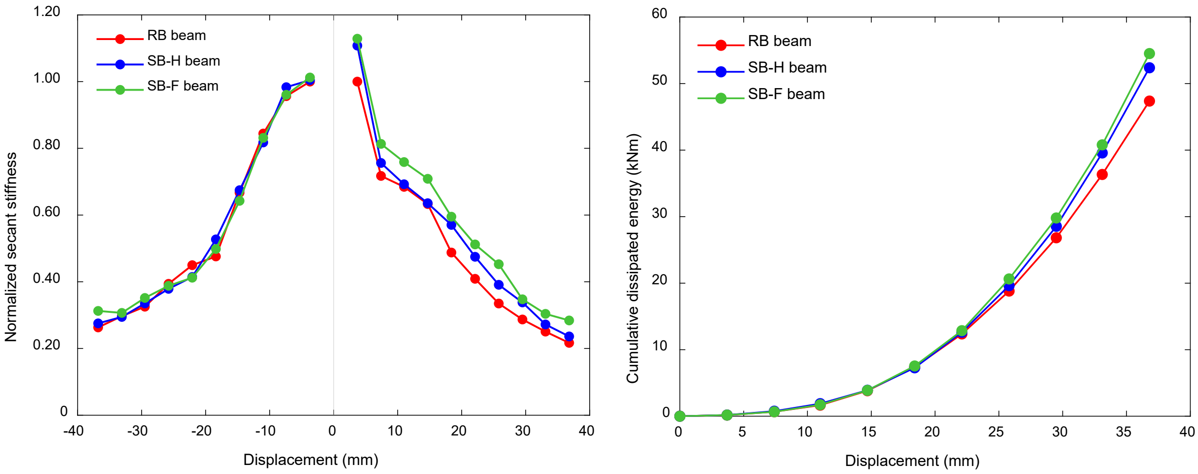

(a) *(b)*

Figure 5: (a) Stiffness degradation, (b) cumulative energy dissipation

3.3 Damage evaluation

This research employs a damage evaluation method inspired by the hysteresis-based energy dissipation framework outlined by Diaz et al. (2017):

$$DI = (1-\eta)E_D(\delta)_{NN} + \eta E_S(\delta)_{NN} \quad (1)$$

where $E_D(\delta)_{NN}$ and $E_S(\delta)_{NN}$ are the normalized functions of dissipated energy and strain energy from the hysteresis loops, respectively, and are determined using the following equations:

$$E_D(\delta)_{NN} = \begin{cases} 0 & 0 \le \delta \le \delta_y \\ \dfrac{\sum E_D(\delta)}{\sum E_D(\delta_u)} & \delta_y \le \delta \le \delta_u \end{cases} \quad (2)$$

$$E_S(\delta)_{NN} = \begin{cases} 0 & 0 \le \delta \le \delta_y \\ \dfrac{E_S(\delta)}{E_S(\delta_u)} & \delta_y \le \delta \le \delta_u \end{cases} \quad (3)$$

where $\Sigma E_D(\delta)$ and $E_D(\delta)$ denote the cumulative dissipated energy and maximum strain energy at a specific displacement stage (δ); $\Sigma E_D(\delta_u)$ and $E_s(\delta_u)$ denote the cumulative dissipated energy and the maximum strain energy at the ultimate displacement (δ_u); and δ_u and δ_y denote the ultimate and yield displacement, respectively.

The DI serves as a measure of structural condition, ranging from 0, indicating an undamaged state, to 1, signifying total collapse, as determined by the failure displacement from the skeleton curve. Figure 6 provides a comparative overview of damage index trends across all specimens relative to cyclic loading displacement. Notably, the strengthened beams sustained less damage than the RB beam, with disparities becoming more evident at larger displacement levels.

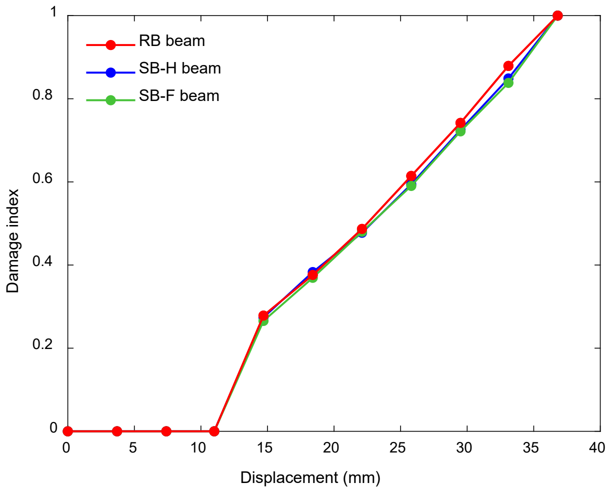

Figure 6. Damage index of tested beams

4 ANALYTICAL APPROACH

This part outlines the analytical method introduced by Haryanto et al. (2022) for estimating the bending capacity of RC beams, following the specifications set by ACI 318-19 (ACI Committee 318, 2019) and ACI 440.2R-17 (ACI Committee 440, 2017). Since the available material properties for concrete and steel were static, dynamic properties were estimated using equations to reflect behaviour under specific strain rates. The CEB Model Code (Comité Euro-International du Béton, 1993) provides an empirical equation for the dynamic increase factor (DIF) of concrete's compressive strength based on strain rate:

$$DIF_{fc} = \frac{f_{cd}}{f_c^{'}} = \begin{cases} \left[\dfrac{\dot{\varepsilon}}{\dot{\varepsilon}_s}\right]^{1.026\alpha} & for\ \ \dot{\varepsilon} \le 30s^{-1} \\ \beta\left[\dfrac{\dot{\varepsilon}}{\dot{\varepsilon}_s}\right]^{1/3} & for\ \ \dot{\varepsilon} > 30s^{-1} \end{cases} \tag{4}$$

where f_{cd} is the dynamic compressive strength (MPa), f_c' is the static compressive strength (MPa), $\dot{\varepsilon}$ is strain rate, $\dot{\varepsilon}_s$ is the reference strain rate equal to 30 x 10-6 (s-1), $\alpha = 1/(5 + 9f_c/f_{co}$, $\beta = 10^{6.156\alpha-2}$, and f_{co} is a constant, equal to 10 MPa.

For reinforcement steel, the dynamic yield strength was determined using the JSCE equation (Japan Society of Civil Engineers, 1993) adopted by Fujikake et al. (2009), while Young's modulus remained unchanged:

$$f_{syd} = f_{sys}\left(1.202 + 0.040 \times \log_{10}\dot{\varepsilon}\right) \ge f_{sys} \tag{5}$$

where f_{syd} is the dynamic yield strength at any strain rate and f_{sys} is the static yield strength, and $\dot{\varepsilon}$ is the strain rate. CFRP rod properties were unaffected by strain rate, aligning with findings by Gao et al. (2023).

The peak strain rate at the mid-span longitudinal tensile steel during yielding was 0.428/s, consistent with Adhikary et al. (2012), though their model overestimated the loading rate–strain rate relationship. Concrete strain gauges recorded a consistent pre-cracking strain rate averaging 0.23/s.

Finally, the sectional moment capacity was converted to the ultimate load capacity of a simply supported beam under three-point bending. Table 2 shows strong agreement across specimens, with an average ratio of 0.97, supporting ACI440.2R-17 (ACI Committee 440, 2017) predictions of flexural strength considering rate-dependent material behavior.

Table 2: Comparison of ultimate load from experimental and analytical results.

	Ultimate load (kN)		**Ratio**
Specimen	**Experimental** P_{exp}	**Analytical** P_{cal}	$\frac{P_{cal}}{P_{exp}}$
RB	176.63	183.60	1.04
SB-H	214.13	201.88	0.94
SB-F	231.14	214.43	0.93
Average			0.97

5 CONCLUSION

This study experimentally evaluated RC-T beams strengthened in the negative moment region using CFRP rods with varying embedment depths via the NSM method, while CFRP sheets were incorporated to enhance confinement and shear capacity. Beams with half-embedded rods (SB-H) and fully embedded rods (SB-F) were compared to a control beam (RB). Furthermore, a rate-dependent material formula was developed and successfully validated. The key conclusions are as follows:

- Under high-cyclic loading, SB-H D and SB-F beams showed 21.23% and 30.86% higher ultimate loads, respectively. However, rod debonding contributed to strength degradation and a reduced residual capacity.
- The enhanced shear resistance and confinement effects provided by the CFRP sheets minimized concrete cover spalling at midspan in the strengthened beams, whereas the RB beam exhibited extensive spalling and concrete crushing.
- The SB-H and SB-F beams exhibited greater stiffness throughout cyclic loading, while NSM-CFRP strengthening, along with the enhanced confinement provided by the CFRP sheets, effectively reduced the stiffness degradation observed in RB.
- As displacement increased, SB-H and SB-F exhibited greater energy dissipation than RB. Higher loading rates enhanced cumulative energy dissipation due to increased yield strength.
- The damage index for all beams was calculated based on dissipated energy during reverse cyclic loading. At small displacements, all beams showed a similar pattern, but as displacement increased, RB exhibited higher damage index values than SB-H and SB-F.

- Analytical predictions of flexural strength in the negative moment region aligned well with experimental results using rate-dependent material models.

ACKNOWLEDGMENTS

The authors would like to acknowledge the financial support provided by the National Center for Research on Earthquake Engineering (NCREE), Taiwan. The authors also extend their sincere appreciation for the material support from PT. SIKA Indonesia.

REFERENCES

ACI Committee 318 (2019). *"Building code requirements for structural concrete and commentary"*. ACI 318-19. American Concrete Institute, Farmington Hills, MI, USA.

ACI Committee 440 (2017). *"Guide for the design and construction of externally bonded FRP systems for strengthening concrete structures"*. ACI 440.2R-17. American Concrete Institute, Farmington Hills, MI, USA.

Adhikary SD, Li B and Fujikake K (2012). "Dynamic behavior of reinforced concrete beams under varying sates of concentrated loading". *International Journal of Impact Engineering*, **47**, 24–38.

Comité Euro-International du Béton (1993). *"CEB-FIP Model Code 1990"*. Redwood Books, Trowbridge, Wiltshire, UK.

Diaz SA, Pujades LG, Barbat AH, Vargas YF, Hidalgo-Leiva DA (2017. "Energy damage index based on capacity and response spectra". *Engineering Structures*, **152**, 424–36.

Fujikake K, Li B and Soeun S (2009). "Impact response of reinforced concrete beam and its analytical evaluation". *Journal of Structural Engineering*, **135**(8):938–950.

Gao D, Bao Z, Han W, Wang X, Huang S, Huang L, Chen Q, Zhao H and Xu Y (2023). "Effect of strain rate on tensile properties of carbon fiber-reinforced epoxy laminates with different stacking sequences and ply orientations". *Polymers*, **15**(12), 2711.

Han AL, Hu H-T, Gan BS, Hsiao F-P and Haryanto Y (2022). "Carbon fiber-reinforced polymer rod embedment depth influence on concrete strengthening". *Arabian Journal for Science and Engineering*, **47**, 12685–12695.

Haryanto Y, Han AL, Hu H-T, Hsiao F-P, Gan BS, Nugroho L and Lin C-C (2023). "Impact of non-reversed low cyclic loading on the seismic response of RC T-beams strengthened in the hogging zone using NSM-CFRP rods with different embedment depth". *33rd International Ocean and Polar Engineering Conference*, 19–23 June, Ottawa, Canada, ISOPE-I-23-457, 11pp.

Haryanto Y, Hsiao F-P, Hu H-T, Han AL, Chua AW, Salim F and Nugroho L (2022). "Structural behavior of negative moment region NSM-CFRP strengthened RC T-beams with various embedment depth under monotonic and cyclic loading". *Composite Structures*, **301**, 116214.

Hassan T and Rizkalla S (2002). "Flexural strengthening of prestressed bridge slabs with FRP systems". PCI Journal, 47(1), 76–93.

Japan Society of Civil Engineers (JSCE) (1993). *"Impact behavior and design of structures"*. Tokyo, Japan. (in Japanese).

Sharaky IA, Torres L, Comas J and Barris C (2014). "Flexural response of reinforced concrete (RC) beams strengthened with near surface mounted (NSM) fibre reinforced polymer (FRP) bars". *Composite Structures*, **109**(1), 8–22.

Zhang SS, Ke Y, Chen E, Biscaia H and Li WG (2022). "Effect of load distribution on the behaviour of RC beams strengthened in flexure with near-surface mounted (NSM) FRP". *Composite Structures*, **279**, 114782.